

# Singlet-triplet excitations and long range entanglement in the spin-orbital liquid candidate $\text{FeSc}_2\text{S}_4$

N. J. Laurita,<sup>1</sup> J. Deisenhofer,<sup>2</sup> LiDong Pan,<sup>1</sup> C. M. Morris,<sup>1</sup> M. Schmidt,<sup>3</sup> M. Johansson,<sup>4</sup> V. Tsurkan,<sup>3,5</sup> A. Loidl,<sup>3</sup> and N. P. Armitage<sup>1</sup>

<sup>1</sup>*The Institute for Quantum Matter, Department of Physics and Astronomy, The Johns Hopkins University, Baltimore, MD 21218, USA*

<sup>2</sup>*Institute of Physics, University of Augsburg, 86135 Augsburg, Germany*

<sup>3</sup>*Experimental Physics V, Center for Electronic Correlations and Magnetism, University of Augsburg, D-86135 Augsburg, Germany*

<sup>4</sup>*Department of Materials and Environmental Chemistry, Stockholm University, 10691 Stockholm, Sweden*

<sup>5</sup>*Institute of Applied Physics, Academy of Sciences of Moldova, MD-2028 Chisinau, Republic of Moldova*

(Dated: May 7, 2022)

Theoretical models of the spin-orbital liquid (SOL)  $\text{FeSc}_2\text{S}_4$  have predicted it to be in close proximity to a quantum critical point separating a spin-orbital liquid phase from a long-range ordered magnetic phase. Here, we examine the magnetic excitations of  $\text{FeSc}_2\text{S}_4$  through time-domain terahertz spectroscopy under an applied magnetic field. At low temperatures an excitation emerges that we attribute to a singlet-triplet excitation from the SOL ground state. A three-fold splitting of this excitation is observed as a function of applied magnetic field. As singlet-triplet excitations are forbidden in inversion symmetric pure spin systems, our results demonstrate the non-trivial character of the entangled spin-orbital singlet ground state. Using experimentally obtained parameters we compare to existing theoretical models to determine  $\text{FeSc}_2\text{S}_4$ 's proximity to the quantum critical point. In the context of these models, we estimate that the characteristic length of the singlet correlations to be  $\xi/(\mathbf{a}/2) \approx 8.2$  (where  $\mathbf{a}/2$  is the nearest neighbor lattice constant) which establishes  $\text{FeSc}_2\text{S}_4$  as a SOL with long-range entanglement.

The search for quantum ground states without classical analogs is a central focus of modern condensed matter physics. A spin liquid would be a prime realization of such a ground state [1]. Such systems would possess local magnetic moments, but, due to quantum fluctuations (typically enhanced due to geometric frustration), do not order even at zero temperature. They are proposed to have non-trivial quantum mechanically entangled wavefunctions, with exotic fractionalized excitations. Quantum fluctuations can disorder the orbital degrees of freedom of localized electrons leading to non-classical ground states [2]. In systems with both spin and orbital fluctuations and spin-orbit coupling, a ‘‘spin-orbital liquid’’ (SOL) ground state has been proposed which is characterized by entangled spin and orbital degrees of freedom [3–5] but no long range order.

Recent experiments have shown a SOL phase may exist in the geometrically frustrated A site cubic spinel ( $\text{AB}_2\text{X}_4$ ) compound  $\text{FeSc}_2\text{S}_4$ . In the absence of further interactions, a tetrahedral  $\text{S}_4$  crystal field splits a  $3d$  shell into an upper  $t_2$  orbital triplet and a lower  $e$  orbital doublet. With Hund’s coupling, an  $\text{Fe}^{2+}$  ion in a tetrahedral environment assumes a high spin  $S = 2$  configuration with a lower  ${}^5\text{E}$  orbital doublet ground state and an upper  ${}^5\text{T}_2$  orbital triplet excited state (Fig. 1). The ground state’s two-fold orbital degeneracy is associated with the freedom to place a hole in either  $e$  orbital. Although such orbital degeneracy is often relieved by Jahn-Teller distortions, magnetic susceptibility measurements show that  $\text{FeSc}_2\text{S}_4$  displays Curie-Weiss behavior with  $\Theta_{CW} = -45.1$  K without long range ordering

down to as low as 50 mK [3]. The frustration parameter,  $f = |\Theta_{CW}|/T_N$ , is at least on the order of 1000, one of the largest ever recorded. The orbital degeneracy’s contributions to the specific heat and magnetic entropy have been verified experimentally [3].

The best starting point to understand the SOL is in terms of the effects of spin-orbit coupling  $\lambda_0(\mathbf{L} \cdot \mathbf{S})$  on the local ionic degrees of freedom, where  $\lambda_0$  is the spin-orbit coupling constant. For the ionic case (e.g. neglecting lattice effects) spin-orbit coupling splits the upper orbital triplet into three levels with energies  $\Delta_{CF} - 3\lambda_0$ ,  $\Delta_{CF} - \lambda_0$ , and  $\Delta_{CF} + 2\lambda_0$ , where  $\Delta_{CF}$  is the  ${}^5\text{E} - {}^5\text{T}_2$  splitting [6, 7]. The ground state orbital doublet is unaffected to first order in the spin-orbit coupling. The potentially huge tenfold ground state degeneracy coming from the six  $3d$  electrons in an  $S = 2$  configuration and the orbital doublet are split at second order in the spin-orbit interaction with 5 levels equally separated by  $\lambda = 6\lambda_0^2/\Delta_{CF}$  (Fig. 1). The lowest state is a spin and orbitally entangled singlet [6] with the form

$$\psi_g = \frac{1}{\sqrt{2}} |x^2 - y^2\rangle |S_z = 0\rangle + \frac{1}{2} |3z^2 - r^2\rangle [|S_z = +2\rangle - |S_z = -2\rangle]. \quad (1)$$

The first excited state is a spin-orbital triplet that is predicted to split in a Zeeman-like fashion with  $g$ -factors of  $\pm(1 - 6\frac{\lambda_0}{\Delta_{CF}})$  [6].

It was suggested by Chen et al. [4, 5] that the spin and orbitally entangled character of the wavefunction is pre-

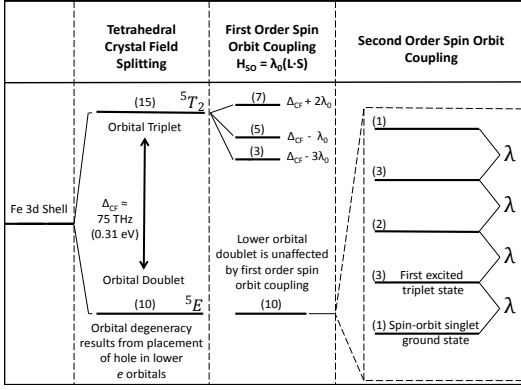


FIG. 1: (a) Energy levels of  $\text{Fe}^{2+}$  ion in an S=2 configuration after tetrahedral crystal field splitting and first and second order spin-orbit coupling, without including lattice effects. Numbers in parenthesis represent the degeneracy of each level. Second order spin-orbit coupling splits the lower  $5E$  doublet into 5 equally spaced levels separated by  $\lambda = 6 \frac{\lambda_0^2}{\Delta_{CF}}$ . The ground state and first excited state form entangled spin-orbital singlet and triplet states.

served when the tetrahedrally coordinated and spin-orbit coupled  $\text{Fe}^{2+}$  ion is incorporated into the  $\text{FeSc}_2\text{S}_4$  lattice. They proposed that the SOL state results from competition between spin-orbital exchange (which favors a magnetically ordered classical ground state) and on-site spin-orbit coupling (which favors a SOL quantum disordered state). In the framework of a mean-field next-nearest neighbor (NNN) Kugel-Khomskii-type “ $J_2/\lambda$ ”-model, in which  $J_2$  is the NNN exchange constant and  $\lambda$  is the excitation energy of single ion  $\text{Fe}^{2+}$  discussed above, Chen et al. predict a quantum phase transition (QPT) at  $x_c = 1/16$  (with  $x = J_2/\lambda$ ) which separates SOL and long range ordered phases. The dominance of NNN exchange in this material is demonstrated by the fact that the lowest energy magnetic excitations are found in neutron scattering at the wavevector for a simple Néel state  $\mathbf{q} = \frac{2\pi}{a}(1, 0, 0)$  [8] and supported by density functional theory which predicts the ratio of NNN to nearest neighbor exchange to be  $\approx 37$  [9]. The SOL differs from the ionic limit in that spin and orbital degrees of freedom may be entangled over longer length scales than just a single site in that a spin on one site becomes entangled with the orbit of another site. Presumably this length scale diverges as the system approaches the QPT. The estimated value for  $x$  was such as to put  $\text{FeSc}_2\text{S}_4$  slightly above the QPT in the magnetically ordered regime [10]. However, the actual proximity to the QPT and even the nature of the ground state has yet to be verified.

Intuitively, one might expect the spectrum of  $\text{FeSc}_2\text{S}_4$  in the SOL phase to be similar to that of the single ion  $\text{Fe}^{2+}$  described above, since the SOL results from degeneracies on individual  $\text{Fe}^{2+}$  and  $\text{FeSc}_2\text{S}_4$  breaks no other symmetries aside from those inherent to the crystal. Chen et al. [4, 5] predicted that while the first excited

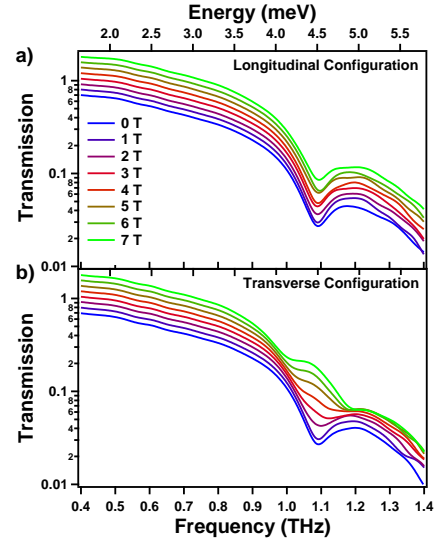


FIG. 2: (a-b) Field dependence of the transmission magnitude of  $\text{FeSc}_2\text{S}_4$  taken at  $T = 5\text{K}$  for the longitudinal (2a) configuration (THz magnetic field  $h_{ac} \parallel H_{dc}$ ) and transverse (2b) configuration ( $h_{ac} \perp H_{dc}$ ). Offsets of 0.05 are included between the curves for clarity.

state would be a triplet, its energy would be substantially renormalized by exchange. In the simplest case with only NNN exchange (e.g. the  $J_2/\lambda$  model) through an expansion in the exchange (valid at  $x \ll x_c$ ) it was shown that the lowest singlet-triplet excitation energy of  $\text{FeSc}_2\text{S}_4$  is

$$E(\mathbf{q}) = \lambda + 2J_2 \sum_A \cos(\mathbf{q} \cdot \mathbf{a}), \quad (2)$$

where  $\mathbf{a}$  represents the lattice vectors of the 12 NNN. Such magnetic excitations can be probed optically through the magnetic dipole interaction. Due to negligible momentum of light compared the lattice scale, in the THz range we probe the  $\mathbf{q} \rightarrow \mathbf{0}$  limit, reducing Eq. 2 to  $E = \lambda(1 + 24x)$ . For  $\text{FeSc}_2\text{S}_4$ , with  $x$  of order the critical value  $1/16$ , one expects the excitation energy to be substantially renormalized from the ionic value.

In this Letter, we use time-domain terahertz spectroscopy (TDTS) to examine the magnetic excitation spectrum of  $\text{FeSc}_2\text{S}_4$ . We find an excitation to a spin-orbit triplet state which splits under an applied static magnetic field,  $H_{dc}$ . Because singlet-triplet excitations are forbidden in inversion symmetric pure spin systems, our results demonstrate the non-trivial character of the entangled spin-orbital singlet ground state and establish  $\text{FeSc}_2\text{S}_4$  as a SOL. Using the  $J_2/\lambda$  model by Chen et al., we make a quantitative connection between the experimentally measured microscopic energy scales of exchange, crystal field, and spin-orbit coupling parameters and the low energy excitations of the system.

Large dense polycrystalline  $\text{FeSc}_2\text{S}_4$  samples were prepared by spark plasma sintering at  $1000^\circ\text{C}$  from precur-

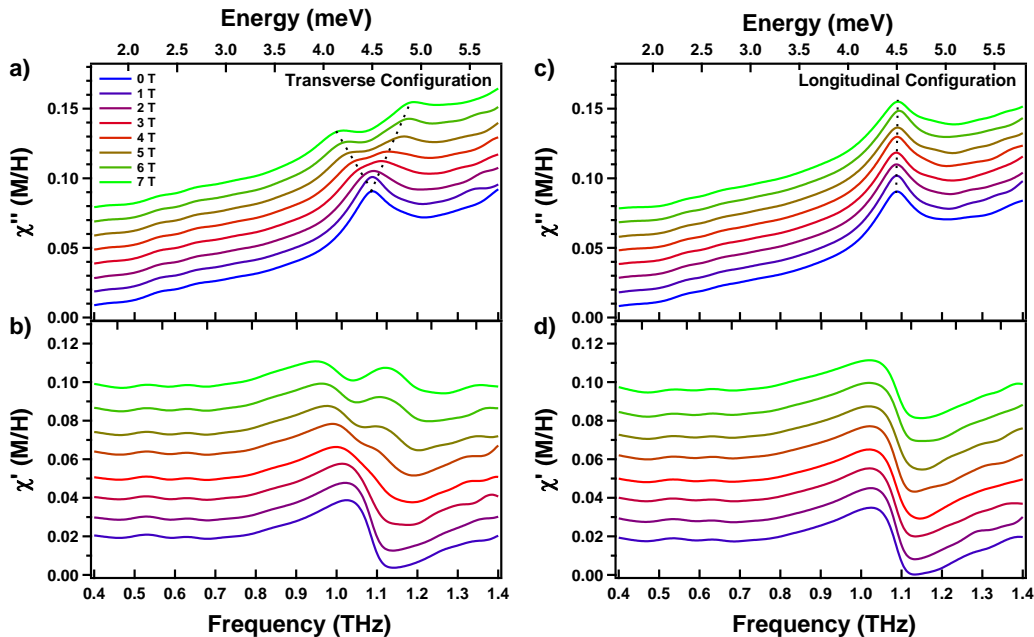


FIG. 3: Field dependence of the imaginary  $\chi''$  and real  $\chi'$  parts of the complex ac susceptibility in the transverse (a-b) and longitudinal (c-d) configurations. All spectra taken at  $T = 5\text{K}$ . The susceptibility is shown in dimensionless SI units and given by the ratio of the magnetization to applied field. Dashed lines are guides to the eye. Offsets of 0.1 are included for clarity.

synthesized binary sulfides  $\text{Sc}_2\text{S}_3$  and  $\text{FeS}$ . Structural, magnetic and optical properties were identical to previous samples prepared by conventional solid state synthesis [3]. The sample was a disc approximately 7.5 mm in diameter and 1 mm thick with a mass of approximately 0.13 g. TDTS transmission experiments were performed using a home built spectrometer with applied magnetic fields up to 7 T in the Voigt geometry (light  $\mathbf{k} \perp \mathbf{H}_{\text{dc}}$ ). TDTS is a high resolution method for accurately measuring the electromagnetic response of a sample in the experimentally challenging THz range. Coupling of the THz fields to magnetic dipole transitions allows access to the frequency dependent *complex* magnetic susceptibility in the zero momentum limit between 100 GHz and 2 THz. Through the use of a double modulated fast rotating polarizer technique [11, 12], we are able to measure the sample's response to two different polarization directions with respect to  $H_{\text{dc}}$  simultaneously. We refer to these as “longitudinal”, in which the THz magnetic field  $h_{\text{ac}} \parallel H_{\text{dc}}$ , and “transverse”, in which  $h_{\text{ac}} \perp H_{\text{dc}}$ . Reflectivity measurements were performed in the mid-infrared frequency range (MIR) from 1000 to 8000  $\text{cm}^{-1}$  using a BRUKER IFS 113v Fourier-transform spectrometer equipped with a He flow cryostat.

Figs. 2a and 2b show the magnitude of the  $T = 5\text{K}$  transmission coefficient as a function of applied field for the longitudinal and transverse configurations. Below 10K, a sharp absorption develops at 1.08 THz ( $\approx 4.5$  meV) in zero field [13]. Its spectral features are constant

below 5K. As we will show below, its energy is in reasonable agreement with the predicted singlet to triplet excitation energy of Eq. 2. Further evidence for this assignment is found in the magnetic field dependence of the transverse configuration. While no splitting is observed in the longitudinal configuration with increasing applied field, the transverse configuration shows a clear splitting into two separate resonances, suggesting the presence of distinct selection rules in the system.

Such a singlet to triplet excitation in typical electron spin resonance measurements is forbidden as the total spin is conserved [14]. Typically, such excitations are only seen in the presence of a Dzyaloshinskii - Moriya interaction or with staggered magnetization arrangements along crystallographic axes. However, neither of these effects can be relevant in  $\text{FeSc}_2\text{S}_4$  due to the inversion symmetric crystal structure. Therefore, the observation of the singlet to triplet excitation is further evidence for the entangled spin-orbital singlet character of the ground state and establishes  $\text{FeSc}_2\text{S}_4$  as a SOL.

In order to better resolve the splitting, the complex ac susceptibility of the sample was calculated from the complex transmission coefficient [15]. Figure 3 shows the field dependence of the calculated imaginary and real parts of the magnetic ac susceptibility for the transverse (3a-3b) and longitudinal (3c-3d) configurations respectively. The splitting of the resonance into two separate features with increasing field is apparent in the transverse configuration. To extract the peak positions for both configura-

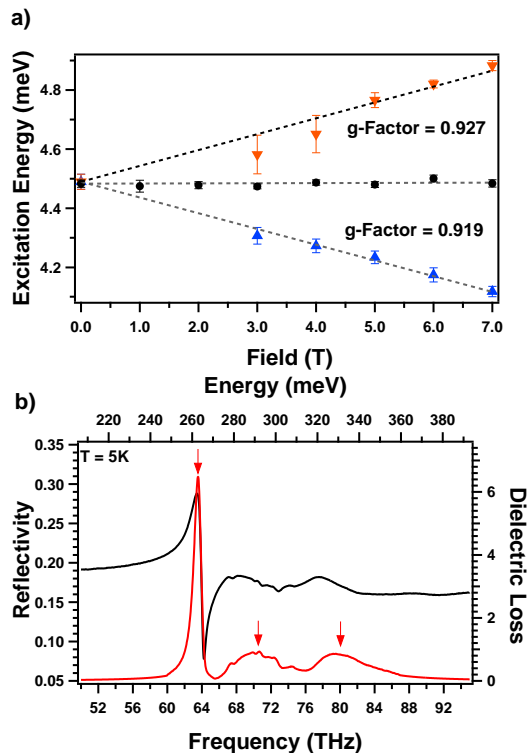


FIG. 4: Excitation energies in the longitudinal and transverse configurations. Error bars are based on the quality of the Lorentzian fits. (b) Mid-infrared reflectivity data taken at  $T = 5\text{K}$  (black, left axis) along with the dielectric loss (red, right axis). Three features are seen with energies of 63.52 THz (0.262 eV), 70.32 THz (0.290 eV), 80.16 THz (0.331 eV) which correspond to the crystal field excitations to the  ${}^5\text{T}_2$  energy levels plus coupling to Jahn-Teller modes of  $\text{Fe}^{2+}$  in a tetrahedral environment.

tions, we fit the spectra with Lorentzian oscillators and a linear background. In related work the linear background has been proposed to derive from a continuum of zone boundary pairs of triplet excitations [13].

Fig. 4a shows the field dependent splitting of the excited state triplet. Quantitative values for the splittings could not be resolved below 3 T. Linear fits were performed on each branch to determine the  $g$ -factors. Only the high field data,  $5\text{T} \leq H \leq 7\text{T}$ , was used in the fitting for the upper branch since lower transmission in the high frequency range causes error below 5 T. All fields were used in the fit for the lower branch. The intercept was forced to coincide with the zero field data for all branches. We find  $g$ -factors of 0.93 and -0.92 for the upper and lower branches respectively.

Mid-infrared reflectivity (MIR) at higher energy was performed in order to determine the crystal field splitting and spin-orbit coupling constant of the sample. Fig. 4b shows the 5K MIR reflectivity (black, left axis) spectrum, which displays a number of prominent features. The excitation energies can be obtained directly by the maxima

of the dielectric loss (indicated by arrows), which was obtained by using a Kramers Kronig consistent variable dielectric function fitting routine [16]. Although one only expects excitations from the  ${}^5\text{E}$  state to the highest and lowest  ${}^5\text{T}_2$  states to be optically active, additional and shifted absorption lines are expected when lattice effects are included due to strong coupling of the  ${}^5\text{T}_2$  levels to vibrational modes [17]. Here it is sufficient to consider only column three of the scheme presented in Fig. 1, as higher order couplings are too small to discern on this scale. Following the approach of Wittekoek et al. [7], the crystal field splitting, spin-orbit coupling constant, Jahn-Teller coupling mode energies ( $E_{JT}$ ), and coupling constants ( $\hbar\omega_{JT}$ ) can be extracted from the mode energies and their intensities. We determine values of  $\Delta_{CF} = 71.6 \pm 5$  THz ( $296.1 \pm 20.7$  meV),  $\lambda_0 = 2.14 \pm 0.15$  THz ( $8.85 \pm 0.62$  meV),  $E_{JT}/\lambda \approx 1.6$ , and  $\hbar\omega_{JT}/\lambda \approx 4$ . From these values we can calculate  $\lambda = 6\lambda_0^2/\Delta_{CF} = 0.38 \pm 0.06$  THz ( $1.57 \pm 0.25$  meV). These values correspond closely to values found in other  $\text{Fe}^{2+}$  tetrahedral compounds [18]. From our experimental value of  $\lambda$  and the value of  $J_2$  [10] extracted from the Curie-Weiss constant, we find from Eq. 2 an expected singlet-triplet energy of 1.31 THz (5.42 meV), which is in reasonable agreement with the observed energy of 1.08 THz.

It was predicted that the  $g$ -factors for  $\text{Fe}^{2+}$  in a tetrahedral configuration go as  $\pm(1 - 6\frac{\lambda_0}{\Delta_{CF}})$  [6]. Substituting in our measured values of  $\lambda_0$  and  $\Delta_{CF}$  gives expected  $g$ -factors of  $\pm 0.82$ , roughly 10% less than the observed value. It may be that corrections to the expression from the  $S = 1$  states would improve this agreement as Hund's coupling in  $\text{Fe}^{2+}$  is expected to be of order  $\Delta_{CF}$  [19]. In this regard, we expect the theoretical prediction to be an underestimation of the experimental value.

With the energy scales characterized, we can work backwards to determine  $\text{FeSc}_2\text{S}_4$ 's proximity to the QPT in the context of the theory of Chen et al. [4, 5]. With an observed excitation energy of 1.08 THz (4.46 meV) and our experimental value for  $\lambda$  we can solve Eq. 2 for  $x$ . Here the implicit assumption is that Eq. 2, which was considered valid far from the critical point as an expansion in the exchange, is still valid near the QPT for momenta far from the ordering wavevector. We find a value of  $x = 0.077$ , which in fact puts  $\text{FeSc}_2\text{S}_4$  slightly above the predicted  $x_c$  of  $x = 1/16$  from mean field theory. The fact that  $\text{FeSc}_2\text{S}_4$  does not order down to the lowest measured temperatures indicates that quantum fluctuations are presumably important in setting the critical value. We may use this value of  $x$  to make an estimate for  $J_2$  of 0.029 THz (0.120 meV), which is about 25% less than the value inferred from the Curie Weiss constant [4, 5, 10].

In this work, we have demonstrated the spin-orbital singlet character of the ground state of  $\text{FeSc}_2\text{S}_4$  through the observation of a singlet-triplet excitation. Its energy is significantly renormalized by the exchange interaction in agreement with the model of Ref. [4, 5]. This sys-

tem, in close proximity to the QPT, presumably differs from a simple ensemble of spin-orbit singlet ions through the presence of longer range correlations. As discussed in Ref. [4, 5], it is believed that the critical regime of this QPT can be described by a Euclidean multicomponent  $\Phi^4$  scalar field theory in 4 space-time dimensions. In such field theories a correlation length can be extracted through the relation  $\xi = \frac{hv}{E}$  where  $E$  is a characteristic energy that vanishes at the QPT and  $v$  is a velocity, whose square is a proportionality between space and time derivatives in the effective Lagrangian. This length can be understood as the scale over which spin and orbital degrees of freedom are entangled. In the present case,  $E \approx 0.17$  meV can be identified with the zone boundary soft gap in neutron scattering [8]. By inspection of the terms in the action written down in Ref. [5], we can identify  $v = \frac{a}{8h} \sqrt{\frac{\lambda^3}{J_2}}$  and find  $\xi = \frac{\lambda a}{8E} \sqrt{\frac{1}{x}}$ . Using our experimentally determined spin-orbit and exchange parameters we estimate a correlation length (in units of the nearest neighbor lattice constant)  $\xi/(a/2) \approx 8.2$ . This demonstrates the long-range entangled character of the SOL non-classical ground state in  $\text{FeSc}_2\text{S}_4$ .

Work at Johns Hopkins was supported by the Gordon and Betty Moore Foundation through Grant GBMF2628, the DOE-BES through DE-FG02-08ER46544, and the ARCS Foundation. In Augsburg this work was supported by the Deutsche Forschungsgemeinschaft via the Transregional Collaborative Research Center TRR 80. We would like to thank L. Balents, G. Chen, J. Kaplan, O. Tchernyshyov, and A. Turner for helpful conversations.

---

[1] L. Balents, *Nature* **464**, 199 (2010).

[2] G. Khaliullin and S. Maekawa, *Phys. Rev. Lett.* **85**, 3950 (2000).

[3] V. Fritsch, J. Hemberger, N. Büttgen, E.-W. Scheidt, H.-A. Krug von Nidda, A. Loidl, and V. Tsurkan, *Phys. Rev. Lett.* **92**, 116401 (2004).

[4] G. Chen, L. Balents, and A. P. Schnyder, *Phys. Rev. Lett.* **102**, 096406 (2009).

[5] G. Chen, A. P. Schnyder, and L. Balents, *Phys. Rev. B*

**80**, 224409 (2009).

[6] W. Low and M. Weger, *Phys. Rev.* **118**, 1119 (1960).

[7] S. Wittekoek, R. P. van Staple, and A. W. J. Wijnma, *Phys. Rev. B* **7**, 1667 (1973).

[8] A. Krimmel, H. Mutka, M. Koza, V. Tsurkan, and A. Loidl, *Physical Review B* **79**, 134406 (2009).

[9] S. Sarkar, T. Maitra, R. Valentí, and T. Saha-Dasgupta, *Physical Review B* **82**, 041105 (2010).

[10] Note that in Ref. [4] there is numerical mistake in the estimate of  $J_2$  from the Curie-Weiss temperature.  $J_2$  should be estimated to be about 45% higher e.g.  $J_2 = 1.9$  K. This would have put the estimated  $x$  for  $\text{FeSc}_2\text{S}_4$  over the predicted mean-field critical value for the transition to the ordered phase.

[11] C. M. Morris, R. V. Aguilar, A. V. Stier, and N. P. Armitage, *Optics Express* **20** (2012).

[12] The setup differed slightly from that in Ref. [11]. Polarizer P1 was set to 45 degrees from the vertical and RP and P2 were placed after OAP 4. P3 was not needed. For a diagonal transmission matrix  $T$ , the in- and out-of-phase lockin outputs in this configuration give a simultaneous measure of  $T_{xx}$  and  $T_{yy}$ . For DC magnetic field polarized in the  $x$  direction this gives the longitudinal and transverse responses simultaneously.

[13] L. Mittelstadt et al., arXiv: **1410.6459** (2014).

[14] T. Sakai, O. Cepas, and T. Ziman, *Physica B: Condensed Matter* **294-295** (2001).

[15] The complex transmission of the sample is given by the relation  $\tilde{T}(\omega) = \frac{4\tilde{Z}}{(\tilde{Z}+1)^2} e^{i\omega(n-1)/d}$ , where  $\tilde{Z} = \sqrt{\frac{\mu}{\epsilon}}$  is the complex impedance,  $d$  is the sample thickness, and  $n = \sqrt{\epsilon\mu}$  is the complex index of refraction. By assuming the magnetic susceptibility,  $\chi$ , is small compared to the dielectric contribution, we can approximate the index of refraction as  $n \approx n(1 + \frac{\chi}{2})$  and the impedance as  $\tilde{Z} \approx \frac{1}{n}$ . The real and imaginary parts of the magnetic ac susceptibility are then  $\tilde{\chi}' = \frac{2}{n} [\frac{c}{d\omega} \text{Arg}(\tilde{T}) + 1 - n]$  and  $\tilde{\chi}'' = \frac{-2c}{d\omega n} [\ln(|\tilde{T}|) - \ln(\frac{4}{n}) + 2\ln(n+1)]$ , where  $\text{Arg}(\tilde{T})$  and  $|\tilde{T}|$  are the phase and magnitude of the complex transmission respectively.

[16] A. B. Kuzmenko, *Review of Scientific Instruments* **76**, 083108 (2005).

[17] G. A. Slack, F. S. Ham, and R. M. Chrenko, *Phys. Rev.* **152**, 376 (1966).

[18] L. F. Feiner, *J. Phys. C* **15** (1982).

[19] G. Chen, private communications (2014).